Stem Cell Research 25 (2017) 72–82

Contents lists available at ScienceDirect

Stem Cell Research

journal homepage: www.elsevier.com/locate/scr

Comparative performance analysis of human iPSC-derived and primary neural progenitor cells (NPC) grown as neurospheres *in vitro*☆

Maxi Hofrichter [a,1], Laura Nimtz [a,1], Julia Tigges [a], Yaschar Kabiri [a], Friederike Schröter [b], Brigitte Royer-Pokora [c], Barbara Hildebrandt [c], Martin Schmuck [a], Alexey Epanchintsev [d], Stephan Theiss [e], James Adjaye [b], Jean-Marc Egly [d], Jean Krutmann [a,f], Ellen Fritsche [a,f,*]

[a] IUF-Leibniz Research Institute for Environmental Medicine, Duesseldorf, Germany
[b] Institute for Stem Cell Research & Regenerative Medicine, Medical Faculty, Heinrich-Heine-University, Duesseldorf, Germany
[c] Institute of Human Genetics, Medical Faculty, Heinrich-Heine University, Duesseldorf, Germany
[d] Department of Functional Genomics and Cancer, Institut de Génétique et de Biologie Moléculaire et Cellulaire: IGBMC, Centre National de la Recherche Scientifique, INSERUM, Université de Strasbourg, Strasbourg, France
[e] Institute of clinical neuroscience and medical psychology, Medical Faculty, Heinrich-Heine-University, Duesseldorf, Germany
[f] Medical Faculty, Heinrich-Heine-University, Düsseldorf, Germany

ARTICLE INFO

Article history:
Received 28 October 2016
Received in revised form 17 October 2017
Accepted 23 October 2017
Available online 26 October 2017

Keywords:
In vitro
Testing
Brain development
Stem cell
MEA

ABSTRACT

Developmental neurotoxicity (DNT) testing performed in rats is resource-intensive (costs, time, animals) and bears the issue of species extrapolation. Thus, reliable alternative human-based approaches are needed for predicting neurodevelopmental toxicity. Human induced pluripotent stem cells (hiPSCs) represent a basis for an alternative method possibly being part of an alternative DNT testing strategy.

Here, we compared two hiPSC neural induction protocols resulting in 3D neurospheres: one using noggin and one cultivating cells in neural induction medium (NIM protocol). Performance of Nestin$^+$/SOX2$^+$ hiPSC-derived neural progenitor cells (NPCs) was compared to primary human NPCs. Generally, primary hNPCs first differentiate into Nestin$^+$ and/or GFAP$^+$ radial glia-like cells, while the hiPSC-derived NPCs (hiPSC-NPC) first differentiate into βIII-Tubulin$^+$ neurons suggesting an earlier developmental stage of hiPSC-NPC. In the 'Neurosphere Assay', NIM generated hiPSC-NPC produced neurons with higher performance than with the noggin protocol. After long-term differentiation, hiPSC-NPC form neuronal networks, which become electrically active on microelectrode arrays after 85 days. Finally, methylmercury chloride inhibits hiPSC-NPC and hNPC migration with similar potencies. hiPSC-NPCs-derived neurospheres seem to be useful for DNT evaluation representing early neural development *in vitro*. More system characterization by compound testing is needed to gain higher confidence in this method.

1. Introduction

Research performed in animals helped understanding physiology and disease and thus lead to the development of treatment strategies over the past decades. However, there seem to be limitations in translation of animal data to humans (Leist and Hartung, 2013), which is one of the discussed causes for failures in drug development (Kenter and Cohen, 2006; Leist and Hartung, 2013; Seok et al., 2013). For this reason, models that resemble human physiology on the molecular level and thus might help predicting drug efficacy and adversity in humans are needed (Leist and Hartung, 2013). Thus, the discovery that differentiated somatic cells can be reprogrammed into human induced pluripotent stem cells (hiPSCs) with the potential to self-renew and differentiate into most cell types of the body (Takahashi et al., 2007) has been raising excitement within the scientific community. Such hiPSCs are human-based and circumvent the ethical issues associated with primary human material or human embryonic stem cells (hESCs) (Kao et al., 2008; Kastenberg and

Abbreviations: BDNF, brain-derived neurotrophic factor; BMPs, bone morphogenic proteins; DNT, Developmental neurotoxicity; EBs, embryoid bodies; GDNF, glial cell line-derived neurotrophic factor; GW, gestational week; hESCs, human embryonic stem cells; hiPSCs, Human induced pluripotent stem cells; hiPSC-NPC, hiPSC-derived NPCs; LOAEC, lowest observed adverse effect concentration; MEA, microelectrode arrays; MeHgCl, methylmercury chloride; nd, not detectable; NDM, neural differentiation medium; NIM, neural induction medium; NPCs, neural progenitor cells; NPM, neural proliferation medium; TGF-β3, transforming growth factor β-3; TTX, tetrodotoxin.

☆ Acknowledgment of grants, equipment, or drugs for research support: This work was funded by iBrain – the interdisciplinary Graduate School for brain research and translational neuroscience at the Heinrich-Heine-University Duesseldorf and CERST-NRW (State Government of Northrhine Westphalia, Germany).

* Corresponding author at: IUF – Leibniz Research Institute for Environmental Medicine, Auf'm Hennekamp 50, DE–40225 Duesseldorf, Germany.
E-mail addresses: ellen.fritsche@iuf-duesseldorf.de, ellen.fritsche@uni-duesseldorf.de (E. Fritsche).

[1] Authors contributed equally.

https://doi.org/10.1016/j.scr.2017.10.013

Odorico, 2008; Singh et al., 2015). Moreover, hiPSCs provide unlimited cell sources, might render the possibility to overcome the species-dependent shortcomings of animal cells and are thus possible alternative models for basic research, disease modeling, drug development and toxicity screening (Robinton and Daley, 2012).

The development of the human brain is a highly complex procedure relying on a large variety of neurodevelopmental processes including proliferation, migration, differentiation, synaptogenesis and apoptosis of neural progenitor cells (NPCs). The need for a spatiotemporally concerted action of such complex processes makes it especially vulnerable to adverse effects of exogenous compounds (Rodier, 1995; Rice and Barone, 2000). Identification of substances with adverse effects on these processes is important, as resulting neurodevelopmental defects may lead to cognitive and intellectual disability as well as to neurological disorders (Grandjean and Landrigan, 2006). These do not only pose a burden on individuals but also provide a socio-economic deficit for society (Bellanger et al., 2013; Trasande et al., 2015).

At present, the gold standards for developmental neurotoxicity (DNT) testing are the rat EPA 870.6300 DNT Guideline (EPA, 1998) and the draft OECD TG426 (OECD, 2007). Performing either one involves high costs (approx. € 1,000,000/compound), takes up to one year and engages a large number of animals. Still there are uncertainties in the guidelines' methodology, evaluation, and regulation (Tsuji and Crofton, 2012). Thus, there is a need for alternative methods evaluating DNT potential of pharmaceuticals and industrial compounds that has been voiced by different stakeholders (Lein et al., 2007; Crofton et al., 2011; Bal-Price et al., 2012, 2015a; Fritsche et al., 2017).

Different *in vitro* methods have been published over the last decade, which evaluate a variety of DNT-related endpoints (Bal-Price et al., 2012, Fritsche et al., 2015). Amongst models from different species (human, mouse, rat) and methods (tumor, primary, stem/progenitor cells), human stem/progenitor cell methods seem to be the most promising as they involve the correct species, resemble physiologically relevant developmental processes and cover a large variety of relevant endpoints (Fritsche et al., 2015). Such methods when based on human embryonic stem cells have the drawback that they are prone to raising ethical concerns when it comes to their usage in compound testing (Kastenberg and Odorico, 2008; Dunnett and Rosser, 2014).

With the goal to overcome the species-dependent and ethical hurdles of current *in vitro* test methods, this study aimed to develop a hiPSC-based neural progenitor cell (hiPSC-NPC) *in vitro* assay based on hiPSC-derived neurospheres that allows assessment of multiple neurodevelopmental endpoints. In addition to assessment of the hiPSC-neurosphere assay performance by comparing two different neural induction protocols, hiPSC-NPCs' performance is compared to primary human NPCs, which are considered as the gold standard for this study (Moors et al., 2009).

2. Material and methods

2.1. hiPSC culture

The hiPSC lines A4, (Wang and Adjaye, 2011), and CRL2097 (characterization in Figs. S1–S6) were cultured in mTeSR1 medium (Stemcell Technologies, Germany) under feeder-free conditions on Matrigel (BD Biosciences, Germany). Medium was changed every day and cells were passaged mechanically using a 0.8 mm × 40 mm syringe needle (BD Biosciences, Germany). Both hiPSC lines were regularly tested for the expression of the pluripotency markers (Fig. S7) and their chromosomal integrity (Fig. S2).

2.2. Neural induction

2.2.1. Noggin protocol

Neural induction was performed as previously described (Denham and Dottori, 2011). Briefly, hiPSC colonies with hESC-like morphology (Fig. S8) were treated with induction medium (KoDMEM (Invtirogen, USA); 20% Knockout Serum Replacement (KSR, Invitrogen, USA); 2 mM L-Glutamine (PAA Laboratories GmbH, Germany); 1×10^{-4} M non-essential amino acids (NEAA, Biochrom, Germany); 1×10^{-4} M β-Mercaptoethanol (Invitrogen, USA); 1% Penicillin/Streptomycin (P/S, Pan Biotech, Germany)) without growth factors but with 500 ng/mL noggin (Peprotech, Germany) for 14 days. Afterwards, colonies were cut and cultured in ultra-low-attachment (ULA) plates (Oehmen, Germany) in neural proliferation medium (NPM) consisting of DMEM (Life Technologies, USA) and Hams F12 (Life Technologies, USA; 3:1) supplemented with 1× B27 (Invitrogen GmbH, Germany), 20 ng/mL epidermal growth factor (EGF; Biosource, Germany) and 20 ng/mL basic fibroblast growth factor (bFGF, R&D Systems, Germany) until they formed free-floating three-dimensional neurospheres and were referred to as hiPSC-NPCs which were kept in culture for an additional 28 days before starting experiments (Fig. 1B).

2.2.2. NIM protocol

This neural induction protocol was modified from a previously described one (Hibaoui et al., 2014). Briefly, hiPSC colonies with hESC-like morphology (Fig. S8) were cut and hiPSC clumps were cultured in ULA plates (Oehmen, Germany) in neural induction medium (NIM) consisting of DMEM (Life Technologies, USA) and Hams F12 (Life Technologies, USA; 3:1) supplemented with 1× B27 (Invitrogen GmBH, Germany), 20 ng/mL EGF (Biosource, Germany) and 1× N2 supplement (Invitrogen, Germany) for 7 days as embryoid bodies (EBs). Subsequently, EBs were transferred into new ULA plates with NIM containing 10 ng/mL bFGF (R&D Systems, Germany) for another 14 days. Afterwards, EBs were referred to as hiPSC-NPCs, transferred into new ULA plates (Oehmen, Germany) and cultured as free-floating three-dimensional neurospheres in NPM.

hiPSC-NPCs from both protocols were cultured under these conditions for at least another 28 days before starting experiments (Fig. 1C).

Three neural inductions of each of the Noggin and the NIM protocol were performed as independent experiments.

2.3. hiPSC-NPC and hNPC culture

Primary fetal hNPCs (GW 16–18) were purchased from Lonza Verviers SPRL (Verviers, Belgium) and were kept in culture as passage 0 for 4 weeks after thawing. Primary hNPCs and hiPSC-NPCs were cultured as 3D free-floating spheres in un-coated and ULA 100 mm petri dishes, respectively, in NPM. Medium was changed every 2–3 days. Proliferating neurospheres were passaged using a McIlwaine tissue chopper to cut them into smaller pieces with a diameter of 200 μm (Mickle Laboratory, UK (Fritsche et al., 2011; Baumann et al., 2014)). After chopping, spheres were allowed to recover for 2 days. This procedure was also performed two days prior to experiments to obtain sphere populations of equal sizes.

2.4. Flow cytometry analysis

For FACS analysis 30 hiPSC-NPCs and primary hNPCs spheres each with a diameter of 300 μm were collected. Cells were singularized by incubation with Accutase (Invitrogen, USA) for 20 min at 37 °C and 5% CO_2. Afterwards, cells were fixed with 4% paraformaldehyde (PFA, Sigma Aldrich, Germany) for 30 min at 37 °C and washed with PBS (Life Technologies, USA). Subsequently, cells were permeabilized with 0.1% PBS-T (Triton-X (Sigma Aldrich, Germany) in PBS) at room temperature for 15 min. Finally, cells were stained with anti-Nestin-Alexa647 (BD Bioscience, Germany) and anti-Sox2-PE (BD Bioscience, Germany) in 0.1% PBS-T in the dark at 4 °C for 30 min. Samples were analyzed using a BD FACSCalibur flow cytometer (BD Biosciences, Germany).

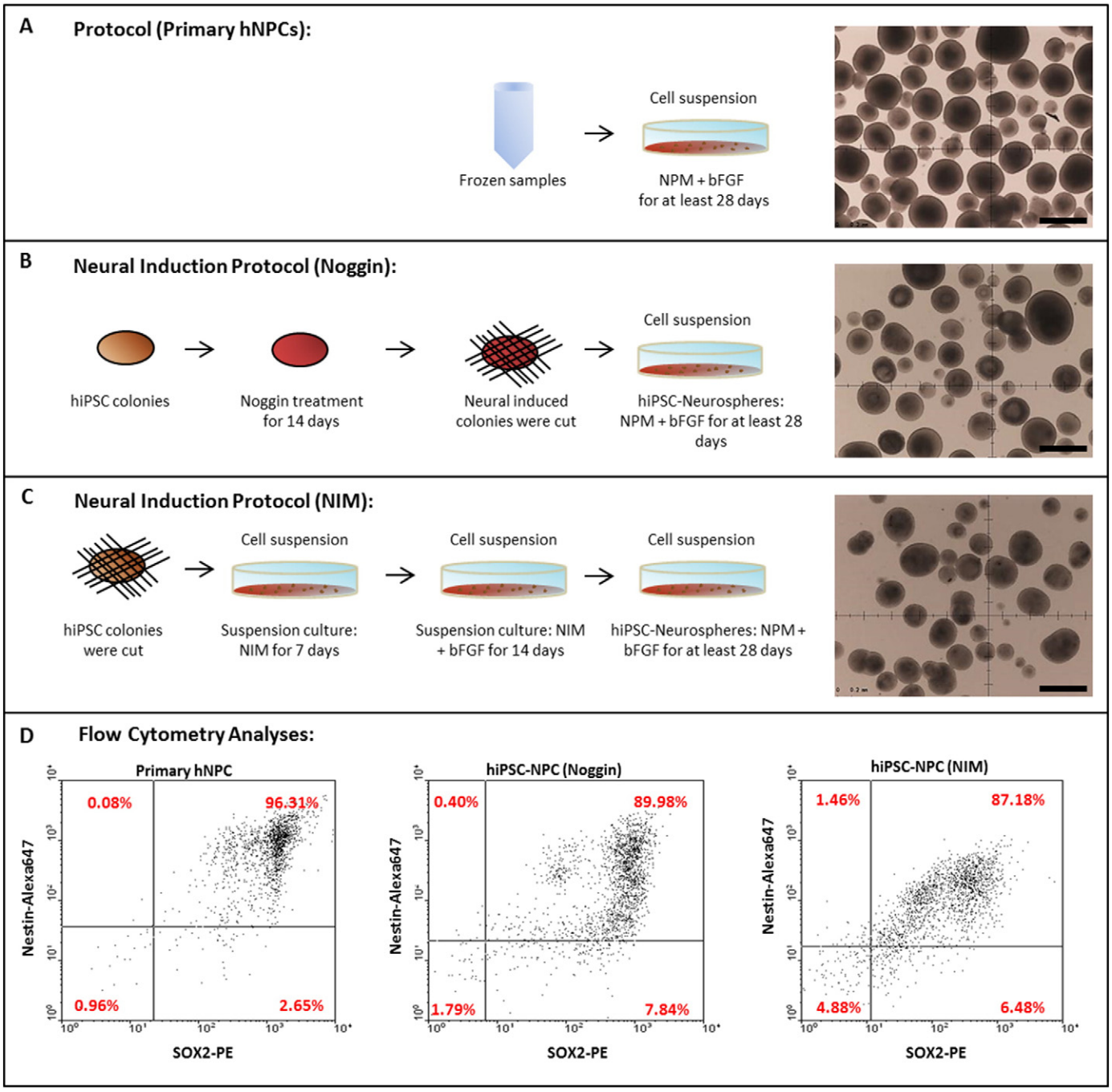

Fig. 1. Neural Induction Protocols to differentiate hiPSCs into neurospheres. hiPSCs were differentiated into neurospheres resembling primary human fetal neurospheres (A) using two different protocols. (B): For the noggin protocol hiPSCs colonies were treated with 500 ng/μL noggin for 14 days. Afterwards they were cut into pieces and cultured as suspension culture in neural proliferation medium (NPM) containing basic fibroblast growth factor (bFGF; Denham and Dottori, 2011). (C): For the NIM protocol hiPSC colonies were cut into pieces and directly cultured as suspension culture in NIM. After 7 days, bFGF was added to the culture for additional 14 days. Finally, hiPSC-derived neurospheres were cultured in NPM containing bFGF for at least 28 days (modified from Hibaoui et al., 2014). Scale bars = 500 μm. (D): hiPS-derived neurospheres generated with the Noggin protocol (B) and the NIM protocol (C) were analyzed for their expression of the neural stem/progenitor markers Nestin and SOX2 *via* flow cytometry analyses and compared to primary human neurospheres. Number of analyzed cells = 2000.

2.5. Quantitative reverse-transcription PCR

RNA was isolated using the RNeasy Mini Kit (Qiagen, Germany) according to manufacturer's protocol. For reverse transcription, 300 ng RNA was transcribed into cDNA using the QuantiTect Rev. Transcription Kit (Qiagen, Germany) according to manufacturer's protocol. Quantitative reverse-transcription polymerase chain reaction (qRT-PCR) was performed using the Rotor Gene Q Cycler (Qiagen, Germany) with QuantiTect SYBR green PCR Master Mix (Qiagen, Germany) following manufacturer's instructions. Primer sequences are presented in supplementary Table 1. Analysis was performed with the ddCT method and the detection limit was set to 0.0001/β-actin. Lower expressions are indicated as 'not detectable' (nd).

2.6. Neurosphere assay

2.6.1. Proliferation assay

Six 300 μm neurospheres per condition were placed into 96-well plates (Greiner, Austria) and cultured either in NPM containing 20 ng/mL EGF (Biosource, Germany) and 20 ng/mL bFGF (R&D Systems,

Germany) or in NPM without growth factors for 14 days. Neurospheres were visualized under a light-optical microscope (Olympus, Germany) and photographed (camera: Visitron Systems, Germany) every 3–4 days. Diameter was measured using ImageJ (National Institutes of Health, USA). Medium was changed every 2–3 days during this assay (Baumann et al., 2014).

2.6.2. Migration assay

NPC migration was assessed as described previously (Moors et al., 2007; Baumann et al., 2014, 2016). For detailed description refer to Supplementary material and methods.

2.6.3. Differentiation assay and immunocytochemistry

Five neurospheres per condition with a diameter of 300 μm were plated in neural differentiation medium (NDM) containing DMEM (Life Technologies, USA) and Hams F12 (Life Technologies, USA; 3:1) supplemented with 1× B27 (Invitrogen GmBH, Germany) and 1× N2 supplement (Invitrogen, Germany) and cultured for 7 or 28 days. Medium was changed once a week. Afterwards, cells were fixed with 4% PFA (Sigma Aldrich, Germany) for 30 min at 37 °C and washed with PBS. Cells were stained with the primary antibodies (mouse-anti-βIII-Tubulin and rabbit-anti-GFAP (Sigma Aldrich, Germany)) for 1 h at 37 °C. For the co-staining of neurons and synapses, cells were stained with mouse-anti-βIII-Tubulin and rabbit-anti-PSD-95 (Abcam, UK) or mouse-anti-Synapsin1 (Synaptic Systems, Germany) for 1 h at 37 °C. After washing with PBS, cells were incubated with the secondary antibodies anti-mouse-Alexa-546 (Invitrogen, USA) and anti-rabbit-Alexa488 (Invitrogen, USA) for 30 min at 37 °C. Nuclei were stained with Hoechst33258 (Sigma Aldrich, Germany). Samples were analyzed using a fluorescent microscope (Carl Zeiss, Germany) and the AxioVision Rel.4.8 software (Carl Zeiss, Germany).

2.6.4. Quantification of immunocytocemistry

βIII-Tubulin staining of the obtained fluorescent images (Fig. 3D) was analyzed using a Fiji Macro (Schindelin et al., 2012). Briefly, images were converted to 8-bit and a local background subtraction was performed using the rolling ball method with a radius of 800 pixels. Consequently, thresholds of the images were defined with fixed background values obtained through averaging Otsu threshold values of three images per experiment. Resulting binary images were filtered for particles larger than 100 pixels, to only obtain neuronal structures. Binary images were analyzed for their area, and neurite mass was calculated by dividing this area by the number of cell nuclei present in a given image. Neurite mass is given as μm^2/nucleus.

The total number of synapses, stained for SYNAPSIN-1 or PSD95, which are co-localized with βIII-Tubulin$^+$ neuronal cells (Fig. 4E, F), were analyzed utilizing a self-written script in the Omnisphero software (Schmuck et al., 2017). Two different thresholding methods were used to pre-process βIII-Tubulin staining in the images. In a first step foreground pixels were removed, using the imopen command (https://www.mathworks.com/help/images/ref/imopen.html) with a non-flat structuring element (ball) with different sizes to get an estimation of the uneven background. This background was subsequently subtracted from the image. On this image an adaptive thresholding method was applied (https://www.mathworks.com/matlabcentral/fileexchange/8647-local-adaptive-thresholding). The resulting binary image was used as a mask to only extract areas from the initial thresholded image, located within the mask. Consequently, the image was thresholded with a fixed threshold and calculated with the isodata algorithm (Ball and Hall, 1965). In a second approach, the same initial background corrected images were processed with various edge detecting algorithms (canny, prewitt, sobel, Roberts and log; Canny, 1986; Lim, 1990; Parker, 1997). Resulting binary images of edges were summed. This image was then added to those obtained from the adaptive thresholding and small holes were closed, utilizing the imfill function. PSD95 and SYNAPSIN-1 were also processed by removing the foreground pixel to estimate the background. Consequently, an isodata threshold was applied and large particles, not considered synapses, were filtered out. In a final step all synapses not located on a binary component of the neuron image were removed. As output the area of the binary neuronal components was calculated, as well as the number of synapse particles and the relative density of these particles as a measure of particle per area. Quantified synapses are shown as synapses/neurite area [μm^2].

We calculated the number of synapses co-localizing with βIII-Tubulin positive neurites in relation to the respective neurite area in three representative images of three independent neural inductions.

2.7. Methylmercury chloride (MeHgCl) treatment and viability assay

Neurospheres were plated as described for the migration assay in the presence of the indicated concentrations of MeHgCl dissolved in DMSO or 0.1% DMSO as solvent control in NDM for 24 h. Migration distance was determined as described above and cell viability was assessed using the Cell Titer-Blue® (CTB) Viability Assay (Promega, Germany) according to manufacturer's instructions. Briefly, primary and CRL2097 and A4 hiPSC-based neurospheres were incubated with the CTB solution for 2, 3.5 and 4.5 h before fluorescence (540Ex/590Em) was measured using a multimode microplate reader (Tecan, Switzerland).

2.8. Neuronal network differentiation on microelectrode arrays (MEA)

Recordings of electrical activity were performed using MEAs with a square array of 59 substrate-embedded titanium nitride microelectrodes (30 μm diameter, 200 μm inter-electrode distance), and an internal reference electrode (200/30iR-Ti-gr, Multichannel Systems MCS GmbH, Reutlingen, Germany). MEA chips were coated with PDL (0.1 mg/mL, 500 μL for 48 h at 4 °C; Sigma Aldrich) and after washing and air-drying with a 50 μL-drop of Laminin (0.01 mg/mL, 48 h at 4 °C; Sigma Aldrich). Afterwards, ~200 hiPS-derived neurospheres (100 μm diameter) were seeded onto MEAs and incubated at 37 °C and 5% CO_2 in NDM medium. For tetrodotoxin (TTX) treatment, 1 μM of TTX (Tocris Bioscience, UK) was added directly to the culture during recordings of the MEA. Afterwards, cultures were washed three times with PBS and fresh NDM medium was added. The same MEA was again measured after 48 h.

2.9. MEA recordings

Recordings of each MEA were performed under sterile conditions for 10 min at one-minute intervals. Therefore, MEAs were placed in the MEA-amplifier (MEA 2100-2x60-System, Multichannel Systems, Germany) and equilibrated to 37 °C for 2 min using the TC02 temperature controller (Multichannel Systems, Germany). Recordings were performed with the MC_Rack-Software (MC_Rack, Multichannel Systems, Germany), electrical activity was sampled at 25 kHz and a background noise below 20 μV. To remove baseline variations, high- and lowpass filters (MCS Filter V 1.0.7, Multichannel Systems, Germany) with cut-off frequencies of 100 Hz and 3500 Hz, respectively, were used. Recordings were analyzed by SpAnNer Software (SpAnNer XBD 3.6, Result GmbH), which detected spikes with a threshold of 8.0 times the standard deviation of the baseline noise level.

2.10. Statistics

All statistical analyses were performed using GraphPad Prism 6.00 for Windows (GraphPad Software, La Jolla Carlifornia USA, www.graphpad.com). To compare different groups of PCR analyses an unpaired *t*-test was performed (Fig. 2A–C). All other data were analyzed using a two-way ANOVA followed by Bonferroni test to correct for multiple testing.

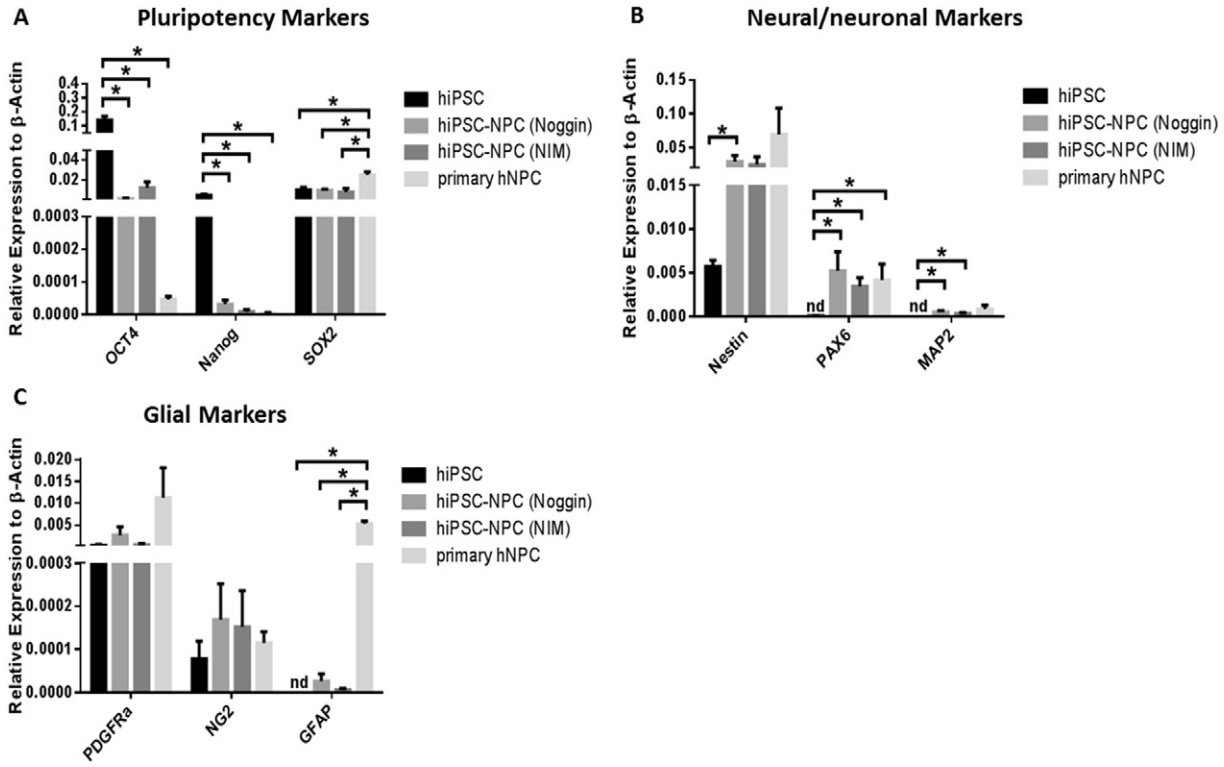

Fig. 2. qRT-PCR analyses of proliferating hiPSC-derived NPCs. hiPSC-derived proliferating neurospheres generated with the noggin and the NIM protocol were analyzed for their mRNA expression profile regarding pluripotency (A; Oct4, Nanog, Sox2), neural/neuronal (B; Nestin, Pax6, Map2) and glial (C; PDGFRα, NG2, GFAP) markers using qRT-PCR analysis. Gene expressions of hiPSC-derived NPC are compared to expressions of these markers in undifferentiated hiPSCs and primary hNPCs. Values are depicted with ddCT method as mean + SEM of relative marker expression to β-actin, n = 3; each n represents data from an independent neural induction. Statistical significance was calculated using the unpaired *t*-test; * significant difference compared to undifferentiated hiPSCs ($p < 0.05$). # significant difference compared to primary hNPCs ($p < 0.05$). nd = not detected (>0.0001/β-actin).

3. Results

3.1. Generation of NPCs from hiPSCs

Two different neural induction protocols were used to create 3D neurospheres consisting of NPCs from hiPSCs. For the first approach hiPSCs were treated with 500 ng/mL noggin (referred to as noggin protocol Denham and Dottori, 2011; Fig. 1B), a protein playing a crucial role in neurogenesis by inhibition of bone morphogenic proteins (BMPs; Lamb et al., 1993; Moreau and Leclerc, 2004). The second protocol was based on a serum-free neural induction medium (referred to as NIM protocol; modified from Hibaoui et al., 2014; Fig. 1C) containing B27 and N2 supplements without additional SMAD inhibitors. Both protocols were tested in two different hiPSC lines, A4 (Wang and Adjaye, 2011) and CRL2097 (Fig. S1–S6) and resulted in free-floating aggregates with spheroid morphology comparable to primary fetal human neurospheres (Moors et al., 2009; Fig. 1A–C).

3.2. Characterization and comparison of proliferating hiPSC-NPCs to primary hNPCs

To ensure that resulting hiPSC-spheres consisted of NPCs, proliferating spheres were singularized and analyzed for the expression of the neural stem cell/progenitor markers Nestin and SOX2 using flow cytometry analyses. Primary hNPCs were analyzed in parallel (Fig. 1D). Almost 100% of primary hNPCs were double-positive for both markers (Fig. 1D). In comparison, hiPSC-NPCs obtained with the different protocols also consisted of 89.98% and 87.18% (Fig. 1D) of $Nestin^+/SOX2^+$ cells, respectively, and another approx. 8% of the cells were either Nestin or SOX2 positive, indicating that both differentiation protocols successfully produced hiPSC-NPCs.

For molecular characterization of proliferating hiPSC-NPCs in comparison with primary hNPCs and undifferentiated hiPSC cultures, we studied the mRNA expression profiles of the pluripotency genes *OCT4*, *NANOG* and *SOX2*, which are highly expressed in hiPSCs (Takahashi et al., 2007; Warren et al., 2010; Vuoristo et al., 2013). Expectedly, undifferentiated hiPSC expressed the highest amount of *OCT4* mRNA, which was one and several orders of magnitude higher than in hiPSC-NPCs and primary NPCs, respectively (Fig. 2A). This pattern was similar for *NANOG* mRNA expression (Fig. 2A). In case of *SOX2*, which is a pluripotency and an NPC marker (Breier et al., 2010; Zhang and Cui, 2014), expression did not change during neural induction of hiPSC in accordance with our expectations. The statistically significant difference of *SOX2* mRNA expression between hiPSC-NPCs and hNPC, however, most likely has no biological relevance as expressions range in the same order of magnitude (Fig. 2A).

Expression of the NPC marker *Nestin* as well as of the early neuroectodermal marker *PAX6* and the advanced neuronal maturation marker *MAP2* (Fig. 2B) were analyzed as neural/neuronal markers. *Nestin* expression was very low in undifferentiated hiPSCs (~0.006/β-actin), but increased after neural induction in both hiPSC-NPCs reaching an expression level similar to primary hNPCs (Fig. 2B). A similar gene expression pattern was detected for *PAX6* and *MAP2*, which were not detectable (nd; <0.0001/β-actin) in undifferentiated hiPSCs, but up-regulated in both hiPSC-NPCs to levels comparable to primary hNPCs (Fig. 2B). Expression of the neuronal marker *MAP2* was not detectable in hiPSCs whereas it was measurable in both hiPSC-NPCs and primary hNPCs just above the detection limit (>0.005/β-actin; Fig. 2B).

The expression profile of glial markers (*PDGFRα*, *NG2*, *GFAP*; Fig. 2C) revealed very low abundance compared to pluripotency or neuronal markers. Markers for oligodendrocyte progenitor cells, *PDGFRα* and *NG2*, were similarly expressed in both hiPSC-NPCs compared to undifferentiated hiPSCs and in primary hNPCs (Fig. 2C). The astrocyte marker

GFAP was not detectable in undifferentiated hiPSCs and just above the detection limit in hiPSC-NPCs, whereas it was well detectable in primary hNPCs (Fig. 2C). Taken these results together, hiPSC-NPCs and primary hNPCs exert a similar gene expression regarding neural and neuronal markers. However, expression of the glial marker *GFAP* revealed a difference between hiPSC-NPCs and primary hNPCs.

3.3. hiPSC-NPCs mimic the main processes of neurodevelopment

The previously established 'Neurosphere Assay' (Fig. 3A) studies compounds' effects on hNPC proliferation, migration and differentiation (Moors et al., 2007, 2009; Gassmann et al., 2010; Baumann et al., 2015). Hence, here we evaluated these endpoints in a comparative study by using primary hNPC and hiPSC-derived NPC generated by two different protocols, NIM and noggin.

Monitoring neurosphere size over time (14 days) revealed that hiPSC-neurospheres from the NIM protocol exhibited similar proliferative capacity compared to primary human neurospheres resulting in a diameter increase of 550 μm and 450 μm, respectively, whereas hiPSC-neurospheres from the noggin protocol proliferated less, resulting in a diameter total increase of approximately 300 μm (Fig. 3B).

The migration assay revealed that after 3 days hNPCs as well as hiPSC-NPCs covered a migration distance of approximately 700 μm (Fig. 3C).

To assess the neuronal differentiation potential of hiPSC-NPCs compared to primary hNPCs, neurospheres were stained cells for the neuronal marker βIII-Tubulin after 7 days of differentiation. All neurospheres were able to differentiate into βIII-Tubulin$^+$ neurons (Fig. 3D), but in contrast to primary human neurospheres and hiPSC-neurospheres from the NIM protocol, the noggin protocol resulted in neurons with weaker βIII-Tubulin staining (Fig. 3D). Moreover, quantification of the

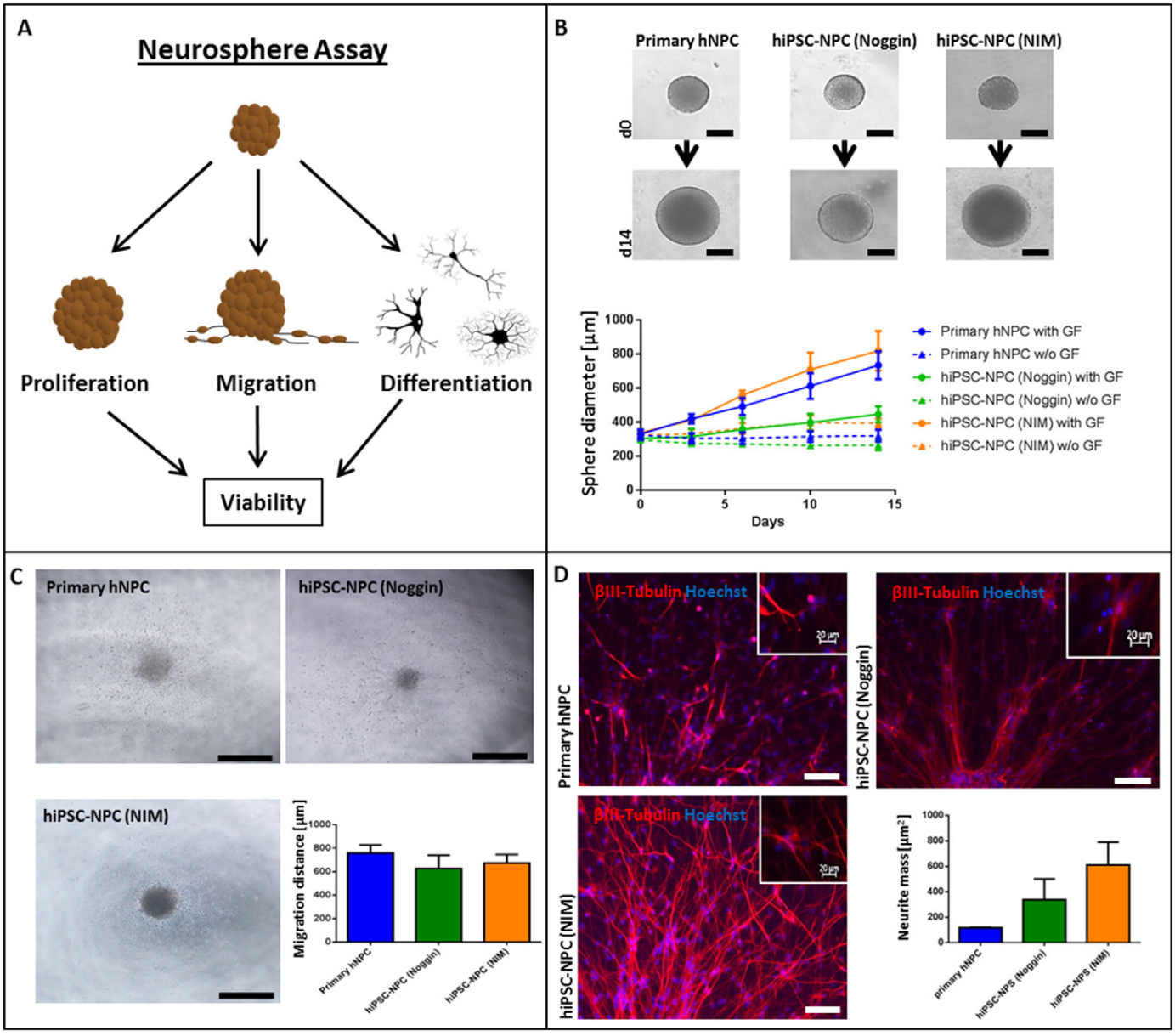

Fig. 3. Comparative functional analyses of hiPSC-neurospheres and primary human neurospheres using the 'Neurosphere Assay'. (A): The 'Neurosphere Assay' is a method to determine basic processes of neurodevelopment (proliferation, migration, differentiation and viability) *in vitro*. (B): Proliferation was measured for 14 days in neural proliferation medium (NPM) with (solid line) or without growth factors (GF; dotted line). Values represent mean ± SD, n = 3. Scale bars = 200 μm. (C): Migration distance of migrating cells 3 days after plating of neurospheres on Poly-D-Lysin (PDL)/Laminin coated plates in NDM. Values represent mean + SEM, n = 3. Scale bars = 500 μm. (D): Immunocytochemical stainings and quantification of at least five representative immunocytochemical images per neural induction for the neuronal marker βIII-Tubulin in 7 days differentiated NPCs of different origins plated on PDL/Laminin coated plates in NDM. Nuclei were stained with Hoechst 33258 (blue). Each n represents an independent neural induction; Scale bars in large images = 100 μm; scale bar in insertions = 20 μm.

immunocytochemical stainings might suggests that hiPSC-neurospheres generated with the NIM protocol contain a larger area of βIII-Tubulin$^+$ neurite staining than primary hNPC or hiPSC-NPC generated with the noggin protocol (Fig. 3D). In addition, the images from the cultures derived from the noggin protocol reveal a higher number of condensed nuclei indicating spontaneous apoptosis (insertions of Fig. 3D). The displayed image is a representative example for this finding.

Taken together these results show that the NIM protocol results in hiPSC-neurospheres, which better resemble primary human neurospheres and display more promising neuronal differentiation than spheres generated with the noggin protocol. Therefore, all following experiments were performed using the NIM protocol.

3.4. hiPSC-NPCs are able to differentiate into functional neuronal networks with spontaneous electrophysiological activity

After 28 days of differentiation, immunocytochemical staining revealed βIII-Tubulin$^+$ neurons and GFAP$^+$ astrocytes in primary as well as hiPSC-neurospheres (NIM; Fig. 4A + B). In contrast to primary hNPC, neurons of hiPSC-neurospheres built a dense neuronal network possibly indicating a higher neuronal maturation state (Fig. 4C, D). This observation is supported by immunocytochemical stainings for the pre-synaptic marker SYNAPSIN-1 and the post-synaptic marker PSD-95, of which the quantification of the staining (Fig. 4G) reveals an approximately similar number of SYNAPSIN-1 and PSD95-positive dots/neurite area: whereas hiPSC-derived neurons co-stain for βIII-Tubulin and SYNAPSIN-1 or PSD-95 (Fig. 4E, F), neurons of primary NPCs are negative for these markers (Fig. S9).

In order to study the functionality of these neuronal networks, hiPSC-neurospheres were cultivated on MEAs in NDM for up to 6 months. The first spontaneous electrophysiological signals were measured after 3 weeks of differentiation (data not shown). After 85 days multiple single spikes were detected (Fig. 5A), indicative of an immature neuronal network. A detailed analysis revealed the typical morphology of monophasic spikes characteristic for physiological action potentials (Fig. 5B, C). Additionally, hiPSC-derived neuronal networks were

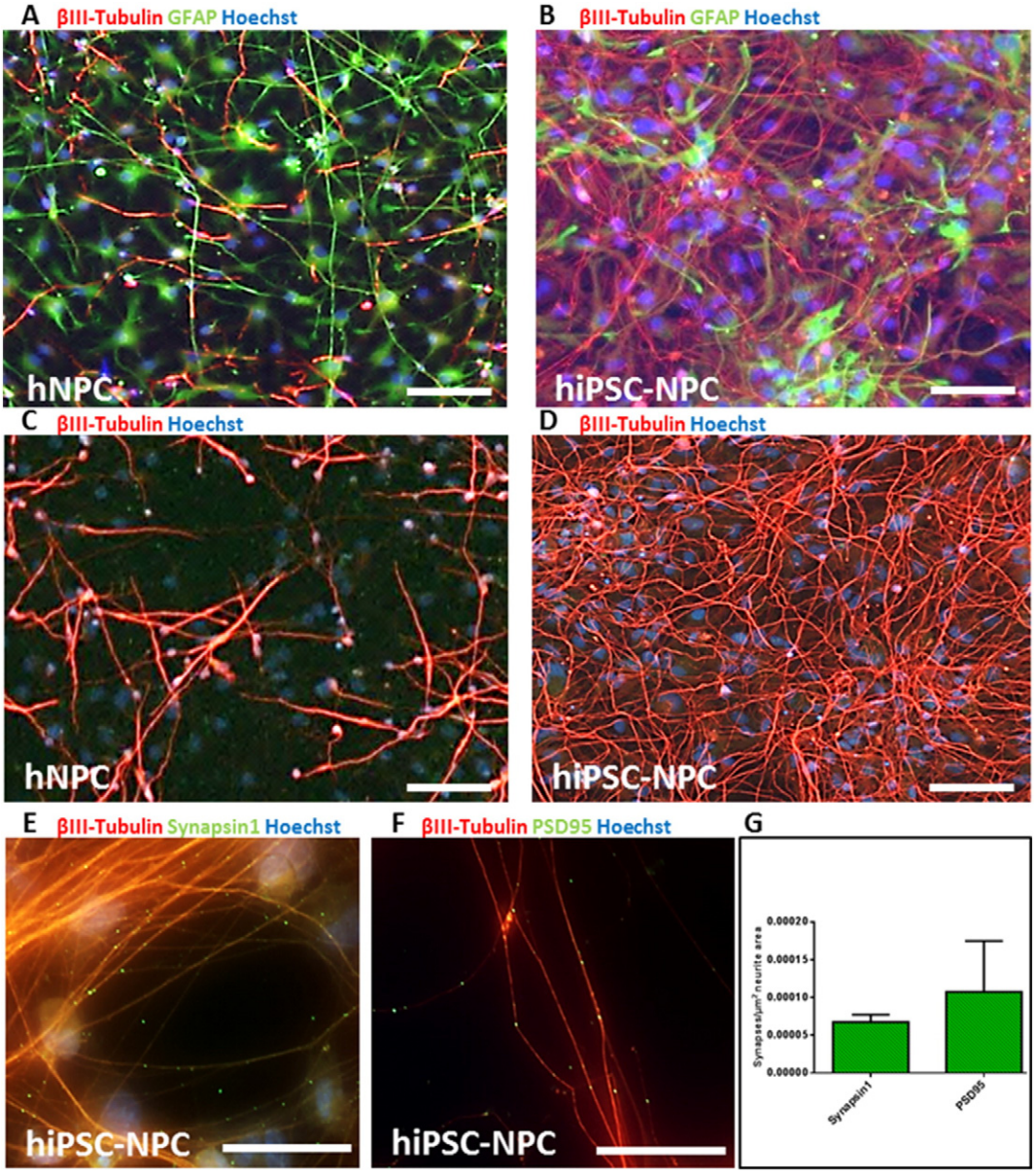

Fig. 4. Comparative immunofluorecent stainings of 28-days differentiated neurospheres. Primary hNPCs (A/C) and hiPSC-NPCs (B/D) were stained for βIII-Tubulin (neurons, red, A–D) and GFAP (astrocytes/NPCs, green, A/B) after 28 days of differentiation. hiPSC-NPCs show co-localization of βIII-Tubulin (red) with the synapse markers Synapsin1 (green, (E)) and PSD-95 (green, (F)) and three representative images of results from three independent neural inductions were quantified (G). Nuclei are counter-stained with Hoechst 33,258. Scale bars A–F = 100 μm.

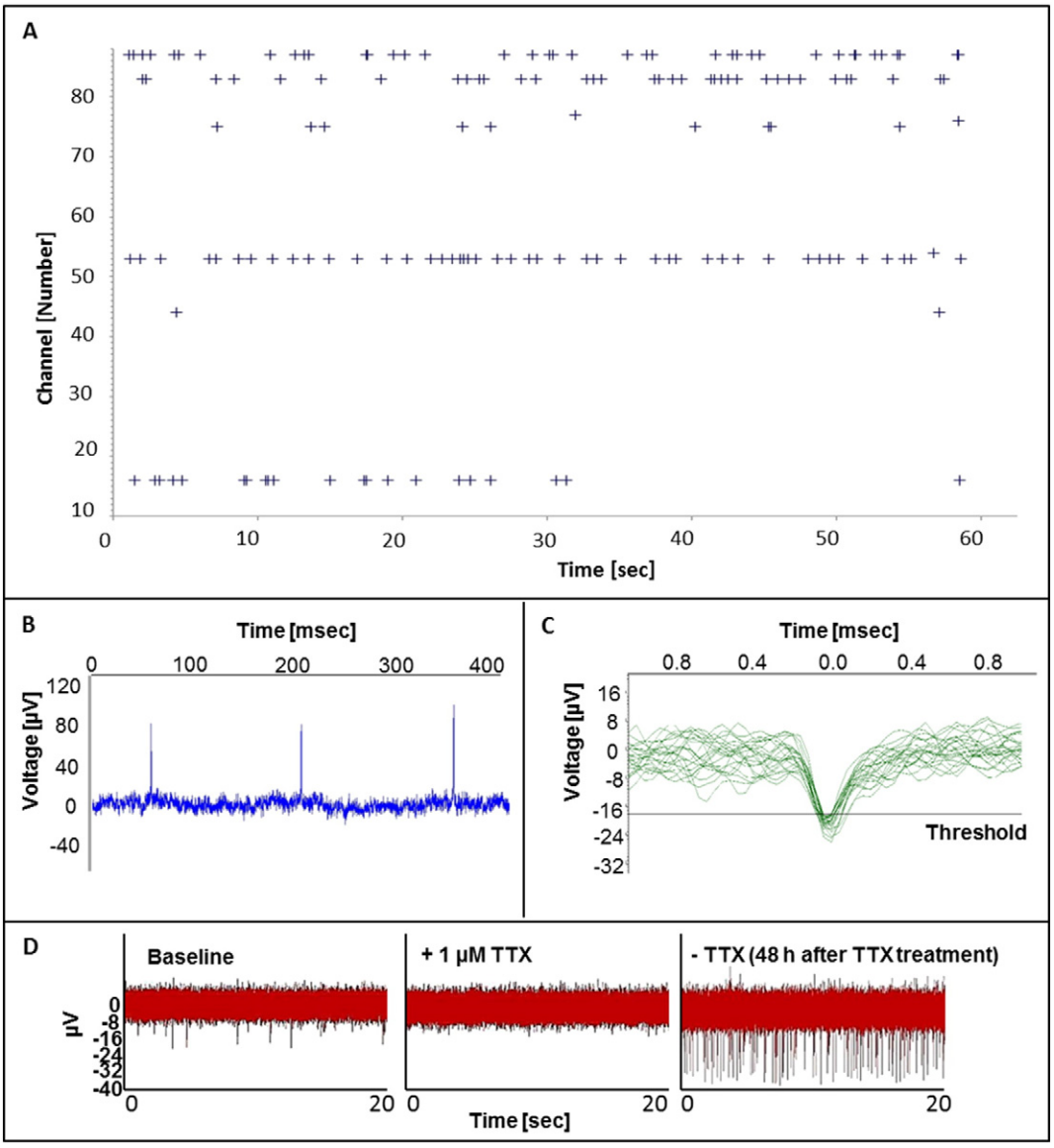

Fig. 5. Electrophysiological activity of hiPSC-derived neuronal networks grown on MEAs. (A): Representative spike raster plot of hiPSC-NPCs differentiated for 85 days on a MEA. Each cross denotes a spike representing an action potential. (B): Spike train of hiPSC-NPCs after 82 days of differentiation. (C): Detected spikes after 85 days of differentiation in a spike overlay. Depicted is one representative out of 7 electrically active chips. (D): After treatment with 1 µM TTX no action potentials (APs) were detected in a hiPSC-NPCs culture differentiated on MEAs for 84 days. After removal of TTX the networks recovered after 48 h resulting in APs with higher frequency and higher amplitude.

sensitive to TTX, demonstrating that the electrophysiological activity in our culture was sodium ion channel-dependent (Lee and Ruben, 2008). This blockage was reversible, as action potentials increased in number and magnitude after a 48 h recovery period in NDM (Fig. 5D), pointing to an adaptive mechanism like homeostatic plasticity.

3.5. hiPSC-NPCs identify disturbances of migration by MeHgCl

To determine if the hiPSC-neurospheres generated with the NIM protocol are a useful model for DNT *in vitro* testing, we performed a proof-of-principle study by treating primary human and hiPSC-derived neurospheres with the DNT model compound MeHgCl (Kadereit et al., 2012). This compound causes mental retardation and developmental delay in children exposed *in utero* (Grandjean and Landrigan, 2006, 2014). DNT of MeHgCl is amongst others due to its inhibition of cell migration resulting in global brain disorganization (Schettler, 2001). Using the 'Neurosphere Assay' we showed that MeHgCl exposure inhibited hNPC migration *in vitro* (Moors et al., 2007, 2009; Baumann et al., 2015). In this study, exposure to increasing concentrations of MeHgCl for 24 h decreased migration distance and viability of hiPSC-derived and primary human neurospheres in a concentration-dependent manner (Fig. 6) with a lowest observed adverse effect concentration (LOAEC) for migration of 0.3 µM MeHgCl for both cell types, whereas the LOAEC for viability was 3 and 1 µM, respectively (Fig. 6A, B). Despite similar LOAECs for migration inhibition, EC_{50} values differed between hiPSC-derived NPC (0.39 µM) and primary hNPC (0.77 µM) for this endpoint, while EC_{50} values for viability did not differ significantly from each other (2.74 and 2.35 µM, respectively, Table 1).

4. Discussion

Fetal hNPCs cultured as neurospheres represent a valuable model for studying neurodevelopmental processes (Svendsen et al., 1998) and thus we have been establishing the hNPC-based 'Neurosphere Assay' (Fig. 3A) as an alternative method for analyzing neurodevelopmental toxicity *in vitro* (Moors et al., 2007, 2009; Gassmann et al., 2010; Baumann et al., 2015). Timing is an important trait during development, thus a possible *in vitro* testing strategy should cover different stages of

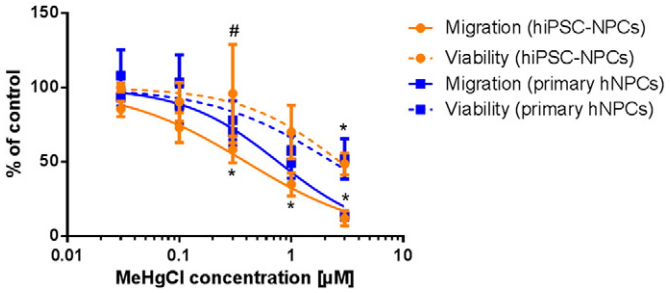

Fig. 6. Effect of the DNT model compound MeHgCl on neurosphere migration. Primary hNPCs and hiPSC-NPCs were treated with different concentrations of MeHgCl (30 nM – 3 µM) for 24 h. Migration distance (solid lines) and viability (dotted lines) were measured. Comparison of MeHgCl effects on migration and viability of primary hNPCs (blue) and hiPSC-NPCs (NIM; orange). Data is presented as concentration-response curve fits and is plotted for comparison of endpoints between cell systems. * significant difference compared to the respective control. # significant difference between the two measured endpoints. All values represent mean ± SD, n = 3; each n represents data from an independent neural induction, $p < 0.05$.

development. Therefore, we set up a hiPSC-NPC 'Neurosphere Assay', which we compared to primary human neurospheres (Fig. 3) as we expected these cells to closer resemble the embryonic period.

hiPSCs bear great potential for future research, as they (i) provide unlimited human cell material, (ii) do not provide the ethical concerns of hESCs and (iii) hold the possibility for human compound hazard assessment and disease modeling (Hatakeyama and Goto, 2016; Mlody et al., 2016; Xie and Tang, 2016). Thus, they are thought to be a useful tool for neuropharmacology/−toxicology (Jennings, 2015). There are numerous publications dealing with the differentiation of hiPSCs into the neuroectodermal lineage either under 2D (Espuny-Camacho et al., 2013; Palm et al., 2015) or 3D (Karumbayaram et al., 2009; Mahairaki et al., 2014) culturing conditions. Neural differentiation is induced either through BMP and transforming growth factor β3 (TGFβ3) inhibition, also known as dual SMAD inhibition (Chambers et al., 2009; Denham and Dottori, 2011; Du et al., 2012; Qiang et al., 2013; Naujock et al., 2014), or by N2 and/or B27 medium supplements (Brennand et al., 2011; Lancaster et al., 2013; Hibaoui et al., 2014). In the present study, we reproduced, optimized and compared two differentiation protocols: (i) BMP inhibition *via* noggin (noggin protocol; Denham and Dottori, 2011) and (ii) neural induction *via* N2 and B27 medium supplements (NIM protocol; modified from Hibaoui et al., 2014). Neural induction was performed in a 3D spherical format as cells grown as organoids seem to be closer to the *in vivo* situation than 2D monolayer cultures (Yamada and Cukierman, 2007; Alepee et al., 2014). The cells derived from both differentiation protocols were compared to primary hNPCs derived from fetal brains. Both protocols resulted in free-floating spheres, which were comparable to primary cells with regard to morphology (Fig. 1A–C), expression of neural stem/progenitor markers (Fig. 1D) and the expression profile of pluripotency as well as neural/neuronal markers (Fig. 2A, B). With respect to glial markers hiPSC-NPCs from both protocols resulted in cells, which seem to represent an earlier maturation stage than primary hNPCs (Fig. 2C). These findings are in line with previous studies reporting that hiPSC-NPCs and so-called EZ spheres, which resemble an early hiPSC-derived neural stem cell (NSC) stage, expressed significantly less glial markers, including *GFAP* and *S100β*, compared to primary hNPCs (Shofuda et al., 2013; Sareen et al., 2014). However, these two studies compared hiPSC-derived NPC to primary embryonic hNPCs of GW 10 (Yamane et al., 2011) and 8, respectively, while the primary NPCs used in our study were of later gestation, *i.e.* fetal origin (GW 16–18). That fetal proliferating NPCs express GFAP is probably due to the fact that GFAP-expressing radial glia, which are in fact NPC (Merkle et al., 2004), play a major role in corticogenesis and are thus present in the progenitor cell preparation of GW 16–18 human brains. Because hiPSC-derived NPCs are generated from stem cells, these cells seem to reflect an earlier developmental stage hardly expressing GFAP, but Nestin and SOX2. This is supported by the observation that 72 h after start of migration neurons migrate on top of $GFAP^+/Nestin^+$ and $GFAP^-/Nestin^+$ glia cells in hNPC and hiPSC-derived NPC, respectively (Fig. S10). Glia cell differentiation from stem cells takes longer than neuronal differentiation *in vitro* (Hu et al., 2010) and neurons also arise before glial cells *in vivo* (Kolb and Gibb, 2011). Thus, gene expression analyses of primary fetal hNPC and hiPSC-derived NPC indicate that each model reflects its respective time of development, *i.e.* fetal and embryonic, respectively.

Performing the 'Neurosphere Assay' (Moors et al., 2007; Breier et al., 2010; Gassmann et al., 2010; Fritsche et al., 2011; Gassmann et al., 2012; Baumann et al., 2014, 2015) with hiPSC-derived neurospheres we analyzed basic processes of early brain development (Fig. 3): NPC proliferation and differentiation of hiPSC-NPC generated with the NIM protocol were more similar to primary human neurospheres and more effective than hiPSC-NPC generated with the noggin protocol, which produced neurons with weaker βIII-Tubulin staining (Fig. 3B, D). Therefore, this protocol was used for all further experiments.

To study if neurons differentiated from either neurospheres were functionally active, we differentiated hNPC and hiPSC-derived neurospheres for 28 days and then immunocytochemically stained them for different markers. hiPSC-neurospheres formed neuronal networks consisting of $βIII\text{-}Tubulin^+$ neurons and $GFAP^+$ astrocytes (Fig. 4B, D), which seemed to be more mature, dense and connected than those formed by primary human neurospheres (Fig. 4A, C). This was confirmed by immunocytochemical stainings for the synaptic markers SYNAPSIN1 and PSD-95, which were only present in hiPSC-derived neurospheres (Fig. 4E–G, Fig. S9). This is in line with previous studies, which reported the expression of the pre- and postsynaptic markers SYNAPTOPHYSIN and PSD95 in hiPSC after 4 weeks of differentiation under 2D culturing conditions (Palm et al., 2015).

In hiPSCs-derived neural cultures neuronal activity on MEAs was monitored in form of asynchronous single spikes starting from 3 weeks of differentiation (Fig. 5), whereas no activity could be measured from primary human neurosphere networks (data not shown). Over the whole incubation period of up to 6 months we observed in turn periods with more and periods with less activity (data not shown), but neither increased number of single spikes, nor synchronicity. The data from Heikkilä and co-workers, who worked with hESC-derived neurons (Heikkilä et al., 2009), indicate that our data represents an immature neuronal network. Nevertheless, our hiPSC-derived neuronal networks exhibited positive and negative monophasic spikes (Fig. 5B, C) as previously described (Heikkilä et al., 2009). The same holds true for the spike amplitude of +/− 20–80 µV (Fig.5B, C). Moreover, hiPSC-derived neuronal networks were sensitive to TTX (Fig. 5D), as previously shown by patch clamp analyses (Palm et al., 2015). As TTX is a potent neurotoxin which blocks voltage-gated sodium channels, these data show that the electrophysiological activity of our culture is sodium channel-dependent (Lee and Ruben, 2008). The effect of TTX was reversible as networks started firing again with even higher amplitudes and frequencies after a recovery period. This is in line with the literature, as TTX treatment influences miniature excitatory postsynaptic current amplitude and frequency depending on the culture time *in vitro* (Turrigiano et al., 1998; Wierenga et al., 2006). At this time we can only speculate on the absence of synchronous signals. One possible explanation is insufficient

Table 1
Calculated EC_{50} values for MeHgCl treatment on migration distance and viability.

EC_{50} values	Primary hNPC	hiPSC-NPCs
Migration	0.77 µM	0.39 µM
95% confidence interval (migration)	0.59–0.99 µM	0.30–0.53 µM
Viability	2.35 µM	2.74 µM
95% confidence interval (viability)	1.17–4.73 µM	1.29–5.81 µM

maturation of the neurons differentiated from hiPSC-derived NPCs. Recently, Palm and co-workers reported that hiPSC-derived neurons exhibited presynaptic, but no postsynaptic currents in voltage clamp recordings after 4 weeks of differentiation illustrating an incomplete neuronal network even though both pre- and postsynaptic markers were present (Palm et al., 2015). These observations reflect our data and might indicate that maturation of hiPSC-derived neurons either takes longer compared to hESC-derived neurons or requires special medium supplements. This is in line with recent findings indicating that complete network maturation of commercially available iPSC-derived cerebral cortical neurons takes 20 to 30 weeks (Odawara et al., 2016) and that co-culture with 1% rat astrocytes and 20% rat primary cortical astrocyte-conditioned medium increases the firing rate (Odawara et al., 2014). Additional experiments, *e.g.* supplementation of creatine, cholesterol or estrogen (Brewer et al., 2008) to the medium, are needed to study if hiPSC-neurosphere differentiation on MEAs can also be enhanced to form synchronized neuronal networks. Also, brain-derived neurotrophic factor (BDNF), glial cell line-derived neurotrophic factor (GDNF), TGF-β3, dibutyryl-cAMP (dbcAMP) or ascorbic acid induce neuronal maturation and might lead to synchronous signals in our system (Heikkilä et al., 2009; Palm et al., 2015).

It has recently been suggested that iPSCs could provide 'the future of *in vitro* toxicology' (Jennings, 2015) and there is consensus that alternative *in vitro* methods might be suitable for DNT hazard and potency evaluation (Tsuji and Crofton, 2012; Bal-Price et al., 2015a). Amongst others, the 'Neurosphere Assay' using primary fetal hNPCs (Moors et al., 2009; Gassmann et al., 2010; Fritsche et al., 2011; Baumann et al., 2015) already complies with this approach. In the present study we provide first evidence that hiPSC-NPCs generated with the NIM protocol might be a useful addition to a possible DNT testing strategy as they seem to resemble an earlier stage of brain development. As a-proof-of-principle the DNT-compound MeHgCl, which causes mental retardation and disturbs neural migration in children exposed *in utero* (Choi et al., 1978; Choi, 1986), inhibits hiPSC-derived NPC migration (Fig. 6). IC_{50} values for inhibition of migration and effects on viability were comparable between primary human and hiPSC-neurospheres (Table 1). This is not surprising because MeHgCl's mode of action, interference with SH-groups of proteins and other molecules and production of oxidative stress, which disturbs cytoskeletal function necessary *e.g.* for migration (Bal-Price et al., 2015b), explains similar migration disturbance in both models despite different developmental stages. To better understand the application domain for neural migration analyses using hiPSC-derived NPC, further studies are needed evaluating the functionality of signaling molecules/pathways known to contribute to normal migration like *e.g.* PLCγ1, GDNF-RET, BDNF/TrkB, PDGFR, FGFR, mTORC1 and Reelin-Dab (Lee, 2015; Ohtaka-Maruyama and Okado, 2015; Kang et al., 2016). In addition, chemicals with known DNT activity need to be tested in this system.

5. Summary and conclusion

In this study we show that hiPSC-derived NPC proliferate, migrate and differentiate similarly to primary fetal hNPCs. However, hiPSC-NPC seem to reflect an earlier developmental stage with primarily neuronal and slower glia cell differentiation than fetal hNPC. In addition, neurons differentiated from hiPSC-derived NPC exert measurable electrical activity. These data suggest that the hiPSC-based neurosphere assay might be a tool to complement the primary neurosphere assay for DNT *in vitro* testing by (i) covering an earlier stage of development and (ii) adding the endpoint of neuronal network formation to a potential neurosphere-based DNT testing battery we suggested earlier (Baumann et al., 2015).

Acknowledgments

The authors would like to thank Drs. Marta Barenys, Jenny Baumann, Katharina Dach and Janette Goniwiecha for useful discussions and comments. Furthermore, we thank Gabriele Freyberger from the Institute of Human Genetics of the HHU for technical assistance.

Disclosure of potential conflicts of interest

None.

Appendix A. Supplementary data

Supplementary data to this article can be found online at https://doi.org/10.1016/j.scr.2017.10.013.

References

Alepee, N., Bahinski, A., Daneshian, M., et al., 2014. State-of-the-art of 3D cultures (organs-on-a-chip) in safety testing and pathophysiology. ALTEX 31, 441–477.
Ball, G.H., Hall, D.J., 1965. ISODATA, A Novel Method of Data Analysis and Pattern Classification. Stanford Research Institute, Menlo Park.
Bal-Price, A.K., Coecke, S., Costa, L., et al., 2012. Advancing the science of developmental neurotoxicity (DNT): testing for better safety evaluation. ALTEX 29, 202–215.
Bal-Price, A., Crofton, K.M., Leist, M., et al., 2015a. International STakeholder NETwork (ISTNET): creating a developmental neurotoxicity (DNT) testing road map for regulatory purposes. Arch. Toxicol. 89, 269–287.
Bal-Price, A., Crofton, K.M., Sachana, M., et al., 2015b. Putative adverse outcome pathways relevant to neurotoxicity. Crit. Rev. Toxicol. 45, 83–91.
Baumann, J., Barenys, M., Gassmann, K., et al., 2014. Comparative human and rat "neurosphere assay" for developmental neurotoxicity testing. Curr. Protoc. Toxicol. 59, 12.21 1–24.
Baumann, J., Gassmann, K., Masjosthusmann, S., et al., 2015. Comparative human and rat neurospheres reveal species differences in chemical effects on neurodevelopmental key events. Arch. Toxicol. https://doi.org/10.1007/s00204-015-1568-8.
Baumann, J., Gassmann, K., Masjosthusmann, S., et al., 2016. Comparative human and rat neurospheres reveal species differences in chemical effects on neurodevelopmental key events. Arch. Toxicol. 90, 1415–1427.
Bellanger, M., Pichery, C., Aerts, D., et al., 2013. Economic benefits of methylmercury exposure control in Europe: monetary value of neurotoxicity prevention. Environ. Health 12, 3.
Breier, J.M., Gassmann, K., Kayser, R., et al., 2010. Neural progenitor cells as models for high-throughput screens of developmental neurotoxicity: state of the science. Neurotoxicol. Teratol. 32, 4–15.
Brennand, K.J., Simone, A., Jou, J., et al., 2011. Modelling schizophrenia using human induced pluripotent stem cells. Nature 473, 221–225.
Brewer, G.J., Boehler, M.D., Jones, T.T., et al., 2008. NbActiv4 medium improvement to Neurobasal/B27 increases neuron synapse densities and network spike rates on multielectrode arrays. J. Neurosci. Methods 170, 181–187.
Canny, J., 1986. A computational approach to edge detection. IEEE Trans. Pattern Anal. Mach. Intell. 8 (6), 679–698.
Chambers, S.M., Fasano, C.A., Papapetrou, E.P., et al., 2009. Highly efficient neural conversion of human ES and iPS cells by dual inhibition of SMAD signaling. Nat. Biotechnol. 27, 275–280.
Choi, B.H., 1986. Methylmercury poisoning of the developing nervous system: I. Pattern of neuronal migration in the cerebral cortex. Neurotoxicology 7, 591–600.
Choi, B.H., Lapham, L.W., Amin-Zaki, L., et al., 1978. Abnormal neuronal migration, deranged cerebral cortical organization, and diffuse white matter astrocytosis of human fetal brain: a major effect of methylmercury poisoning in utero. J. Neuropathol. Exp. Neurol. 37, 719–733.
Crofton, K.M., Mundy, W.R., Lein, P.J., et al., 2011. Developmental neurotoxicity testing: recommendations for developing alternative methods for the screening and prioritization of chemicals. ALTEX 28, 9–15.
Denham, M., Dottori, M., 2011. Neural differentiation of induced pluripotent stem cells. Methods Mol. Biol. 793, 99–110.
Du, J., Campau, E., Soragni, E., et al., 2012. Role of mismatch repair enzymes in GAA.TTC triplet-repeat expansion in Friedreich ataxia induced pluripotent stem cells. J. Biol. Chem. 287, 29861–29872.
Dunnett, S.B., Rosser, A.E., 2014. Challenges for taking primary and stem cells into clinical neurotransplantation trials for neurodegenerative disease. Neurobiol. Dis. 61, 79–89.
EPA, U.S., 1998. Health Effects Guidelines OPPTS 870.6300 Developmental Neurotoxicity Study (EPA 712-C-98-239).
Espuny-Camacho, I., Michelsen, K.A., Gall, D., et al., 2013. Pyramidal neurons derived from human pluripotent stem cells integrate efficiently into mouse brain circuits in vivo. Neuron 77, 440–456.
Fritsche, E., Gassmann, K., Schreiber, T., 2011. Neurospheres as a model for developmental neurotoxicity testing. Methods Mol. Biol. 758, 99–114.
Fritsche, E., Alm, H., Baumann, J., Geerts, L., Hakansson, H., Masjosthusmann, S., Witters, H., 2015. Literature Review on In Vitro and Alternative Developmental Neurotoxicity (DNT) Testing Methods. EFSA Supporting Publication EN-778 (186 pp).
Fritsche, E., Crofton, K.M., Hernandez, A.F., et al., 2017. OECD/EFSA workshop on developmental neurotoxicity (DNT): the use of non-animal test methods for regulatory purposes. ALTEX 34, 311–315.
Gassmann, K., Abel, J., Bothe, H., et al., 2010. Species-specific differential AhR expression protects human neural progenitor cells against developmental neurotoxicity of PAHs. Environ. Health Perspect. 118, 1571–1577.

Gassmann, K., Baumann, J., Giersiefer, S., et al., 2012. Automated neurosphere sorting and plating by the COPAS large particle sorter is a suitable method for high-throughput 3D in vitro applications. Toxicol. in Vitro 26, 993–1000.
Grandjean, P., Landrigan, P.J., 2006. Developmental neurotoxicity of industrial chemicals. Lancet 368, 2167–2178.
Grandjean, P., Landrigan, P.J., 2014. Neurobehavioural effects of developmental toxicity. Lancet Neurol. 13, 330–338.
Hatakeyama, H., Goto, Y.I., 2016. Concise Review: heteroplasmic Mitochondrial DNA mutations and mitochondrial diseases: toward iPSC-based disease modeling, drug discovery, and regenerative therapeutics. Stem Cells 34, 801–808.
Heikkilä, T.J., Yla-Outinen, L., Tanskanen, J.M., et al., 2009. Human embryonic stem cell-derived neuronal cells form spontaneously active neuronal networks in vitro. Exp. Neurol. 218, 109–116.
Hibaoui, Y., Grad, I., Letourneau, A., et al., 2014. Modelling and rescuing neurodevelopmental defect of Down syndrome using induced pluripotent stem cells from monozygotic twins discordant for trisomy 21. EMBO Mol. Med. 6, 259–277.
Hu, B.Y., Weick, J.P., Yu, J., et al., 2010. Neural differentiation of human induced pluripotent stem cells follows developmental principles but with variable potency. Proc. Natl. Acad. Sci. U. S. A. 107, 4335–4340.
Jennings, P., 2015. The future of in vitro toxicology. Toxicol. in Vitro 29, 1217–1221.
Kadereit, S., Zimmer, B., van Thriel, C., et al., 2012. Compound selection for in vitro modeling of developmental neurotoxicity. Front. Biosci. (Landmark Ed) 17, 2442–2460.
Kang, D.S., Yang, Y.R., Lee, C., et al., 2016. Roles of phosphoinositide-specific phospholipase Cgamma1 in brain development. Adv. Biol. Regul. 60, 167–173.
Kao, C.F., Chuang, C.Y., Chen, C.H., et al., 2008. Human pluripotent stem cells: current status and future perspectives. Chin. J. Physiol. 51, 214–225.
Karumbayaram, S., Novitch, B.G., Patterson, M., et al., 2009. Directed differentiation of human-induced pluripotent stem cells generates active motor neurons. Stem Cells 27, 806–811.
Kastenberg, Z.J., Odorico, J.S., 2008. Alternative sources of pluripotency: science, ethics, and stem cells. Transplant. Rev. (Orlando) 22, 215–222.
Kenter, M.J., Cohen, A.F., 2006. Establishing risk of human experimentation with drugs: lessons from TGN1412. Lancet 368, 1387–1391.
Kolb, B., Gibb, R., 2011. Brain plasticity and behaviour in the developing brain. J. Can. Acad. Child Adolesc. Psychiatry 20, 265–276.
Lamb, T.M., Knecht, A.K., Smith, W.C., et al., 1993. Neural induction by the secreted polypeptide noggin. Science 262, 713–718.
Lancaster, M.A., Renner, M., Martin, C.A., et al., 2013. Cerebral organoids model human brain development and microcephaly. Nature 501, 373–379.
Lee, d.Y., 2015. Roles of mTOR signaling in brain development. Exp. Neurobiol. 24, 177–185.
Lee, C.H., Ruben, P.C., 2008. Interaction between voltage-gated sodium channels and the neurotoxin, tetrodotoxin. Channels (Austin) 2, 407–412.
Lein, P., Locke, P., Goldberg, A., 2007. Meeting report: alternatives for developmental neurotoxicity testing. Environ. Health Perspect. 115, 764–768.
Leist, M., Hartung, T., 2013. Inflammatory findings on species extrapolations: humans are definitely no 70-kg mice. Arch. Toxicol. 87, 563–567.
Lim, Jae S., 1990. Two-dimensional Signal and Image Processing. Prentice Hall, Englewood Cliffs, NJ (710.p).
Mahairaki, V., Ryu, J., Peters, A., et al., 2014. Induced pluripotent stem cells from familial Alzheimer's disease patients differentiate into mature neurons with amyloidogenic properties. Stem Cells Dev. 23, 2996–3010.
Merkle, F.T., Tramontin, A.D., Garcia-Verdugo, J.M., et al., 2004. Radial glia give rise to adult neural stem cells in the subventricular zone. Proc. Natl. Acad. Sci. U. S. A. 101, 17528–17532.
Mlody, B., Lorenz, C., Inak, G., et al., 2016. Energy metabolism in neuronal/glial induction and in iPSC models of brain disorders. Semin. Cell. Dev. Biol. 52, 102–109.
Moors, M., Cline, J.E., Abel, J., et al., 2007. ERK-dependent and -independent pathways trigger human neural progenitor cell migration. Toxicol. Appl. Pharmacol. 221, 57–67.
Moors, M., Rockel, T.D., Abel, J., et al., 2009. Human neurospheres as three-dimensional cellular systems for developmental neurotoxicity testing. Environ. Health Perspect. 117, 1131–1138.
Moreau, M., Leclerc, C., 2004. The choice between epidermal and neural fate: a matter of calcium. Int. J. Dev. Biol. 48, 75–84.
Naujock, M., Stanslowsky, N., Reinhardt, P., et al., 2014. Molecular and functional analyses of motor neurons generated from human cord-blood-derived induced pluripotent stem cells. Stem Cells Dev. 23, 3011–3020.
Odawara, A., Saitoh, Y., Alhebshi, A.H., et al., 2014. Long-term electrophysiological activity and pharmacological response of a human induced pluripotent stem cell-derived neuron and astrocyte co-culture. Biochem. Biophys. Res. Commun. 443 (4), 1176–1181.
Odawara, A., Katoh, H., Matsuda, N., et al., 2016. Physiological maturation and drug responses of human induced pluripotent stem cell-derived cortical neuronal networks in long-term culture. Sci. Rep. 6, 26181.
OECD, 2007. OECD Guideline for the testing of chemicals. Developmental Neurotoxicity study TG. 426.
Ohtaka-Maruyama, C., Okado, H., 2015. Molecular pathways underlying projection neuron production and migration during cerebral cortical development. Front. Neurosci. 9, 447.
Palm, T., Bolognin, S., Meiser, J., et al., 2015. Rapid and robust generation of long-term self-renewing human neural stem cells with the ability to generate mature astroglia. Sci. Rep. 5, 16321.
Parker, James R., 1997. Algorithms for Image Processing and Computer Vision. John Wiley & Sons, Inc., New York, pp. 23–29.
Qiang, L., Fujita, R., Abeliovich, A., 2013. Remodeling neurodegeneration: somatic cell reprogramming-based models of adult neurological disorders. Neuron 78, 957–969.
Rice, D., Barone Jr., S., 2000. Critical periods of vulnerability for the developing nervous system: evidence from humans and animal models. Environ. Health Perspect. 108 (Suppl. 3), 511–533.
Robinton, D.A., Daley, G.Q., 2012. The promise of induced pluripotent stem cells in research and therapy. Nature 481, 295–305.
Rodier, P.M., 1995. Developing brain as a target of toxicity. Environ. Health Perspect. 103 (Suppl. 6), 73–76.
Sareen, D., Gowing, G., Sahabian, A., et al., 2014. Human induced pluripotent stem cells are a novel source of neural progenitor cells (iNPCs) that migrate and integrate in the rodent spinal cord. J. Comp. Neurol. 522, 2707–2728.
Schettler, T., 2001. Toxic threats to neurologic development of children. Environ. Health Perspect. 109 (Suppl. 6), 813–816.
Schindelin, J., Arganda-Carreras, I., Frise, E., et al., 2012. Fiji: an open-source platform for biological-image analysis. Nat. Methods 9 (7), 676–682.
Schmuck, M.R., Temme, T., Dach, K., et al., 2017. Omnisphero: a high-content image analysis (HCA) approach for phenotypic developmental neurotoxicity (DNT) screenings of organoid neurosphere cultures in vitro. Arch. Toxicol. 91 (4), 2017–2028.
Seok, J., Warren, H.S., Cuenca, A.G., et al., 2013. Genomic responses in mouse models poorly mimic human inflammatory diseases. Proc. Natl. Acad. Sci. U. S. A. 110, 3507–3512.
Shofuda, T., Fukusumi, H., Kanematsu, D., et al., 2013. A method for efficiently generating neurospheres from human-induced pluripotent stem cells using microsphere arrays. Neuroreport 24, 84–90.
Singh, V.K., Kalsan, M., Kumar, N., et al., 2015. Induced pluripotent stem cells: applications in regenerative medicine, disease modeling, and drug discovery. Front. Cell Dev. Biol. 3, 2.
Svendsen, C.N., ter Borg, M.G., Armstrong, R.J., et al., 1998. A new method for the rapid and long term growth of human neural precursor cells. J. Neurosci. Methods 85, 141–152.
Takahashi, K., Tanabe, K., Ohnuki, M., et al., 2007. Induction of pluripotent stem cells from adult human fibroblasts by defined factors. Cell 131, 861–872.
Trasande, L., Zoeller, R.T., Hass, U., et al., 2015. Estimating burden and disease costs of exposure to endocrine-disrupting chemicals in the European union. J. Clin. Endocrinol. Metab. 100, 1245–1255.
Tsuji, R., Crofton, K.M., 2012. Developmental neurotoxicity guideline study: issues with methodology, evaluation and regulation. Congenit. Anom. (Kyoto) 52, 122–128.
Turrigiano, G.G., Leslie, K.R., Desai, N.S., et al., 1998. Activity-dependent scaling of quantal amplitude in neocortical neurons. Nature 391, 892–896.
Vuoristo, S., Toivonen, S., Weltner, J., et al., 2013. A novel feeder-free culture system for human pluripotent stem cell culture and induced pluripotent stem cell derivation. PLoS One 8, e76205.
Wang, Y., Adjaye, J., 2011. A cyclic AMP analog, 8-Br-cAMP, enhances the induction of pluripotency in human fibroblast cells. Stem Cell Rev. 7, 331–341.
Warren, L., Manos, P.D., Ahfeldt, T., et al., 2010. Highly efficient reprogramming to pluripotency and directed differentiation of human cells with synthetic modified mRNA. Cell Stem Cell 7, 618–630.
Wierenga, C.J., Walsh, M.F., Turrigiano, G.G., 2006. Temporal regulation of the expression locus of homeostatic plasticity. J. Neurophysiol. 96, 2127–2133.
Xie, N., Tang, B., 2016. The application of human iPSCs in neurological diseases: from bench to bedside. Stem Cells Int. 2016, 6484713.
Yamada, K.M., Cukierman, E., 2007. Modeling tissue morphogenesis and cancer in 3D. Cell 130, 601–610.
Yamane, J., Ishibashi, S., Sakaguchi, M., et al., 2011. Transplantation of human neural stem/progenitor cells overexpressing galectin-1 improves functional recovery from focal brain ischemia in the Mongolian gerbil. Mol. Brain 4, 35.
Zhang, S., Cui, W., 2014. Sox2, a key factor in the regulation of pluripotency and neural differentiation. World J. Stem Cells 6, 305–311.